

Majorana Fermions and Odd-frequency Cooper Pairs in a Nano Wire

Yasuhiro Asano¹ and Yukio Tanaka²

¹*Department of Applied Physics and Center for Topological Science
& Technology, Hokkaido University, Sapporo 060-8628, Japan*

²*Department of Applied Physics, Nagoya University, Nagoya 464-8603, Japan*

(Dated: November 8, 2018)

We discuss a strong relationship between Majorana fermions and odd-frequency Cooper pairs which appear at a disordered normal (N) nano wire attached to a topologically nontrivial superconducting (S) one. The transport properties in superconducting nano wire junctions show universal behaviors irrespective of the degree of disorder: the quantized zero-bias differential conductance at $2e^2/h$ in NS junction and the fractional current-phase ($J-\varphi$) relationship of the Josephson effect in SNS junction $J \propto \sin(\varphi/2)$. Such behaviors are exactly the same as those found in the anomalous proximity effect of odd-parity spin-triplet superconductors. We show that the odd-frequency pairs exist wherever the Majorana fermions stay.

PACS numbers: 74.25.F-, 74.45.+c, 74.78.Na

Majorana fermion (MF) satisfying a special relation of $\gamma = \gamma^\dagger$ with γ (γ^\dagger) being the annihilation (creation) operator has been an exciting object since the original prediction by Majorana¹. Finding of MFs and controlling of Majorana bound states (MBSs) are hot research issues in condensed matter physics² from the view of potential application of MBS to the topological quantum computation^{3,4}. To date, we have known several promising systems hosting MFs such as spin-triplet p -wave superconductors⁵⁻⁸, topological insulator /superconductor heterostructures⁹ semiconductor / superconductor junctions with strong spin-orbit coupling¹⁰⁻¹³, helical superconductors¹⁴, and superconducting topological insulators¹⁵. Most attracting case among them is the semiconductor nano wire fabricated on top of a superconductor because of its easy tunability of MBS by changing the chemical potential in the nano wire and by applying the Zeeman field onto it^{16,17}. Actually, a plenty of theoretical studies have discussed MFs or MBSs in such nano wires^{18,19}. The zero-bias conductance peak reported very recently would be considered as an evidence of MFs (MBS)^{16,17,20}. These researches have stimulated a number of theoretical investigation on unusual charge transport phenomena through the MBS in normal-metal / superconductor (NS) and superconductor /normal-metal/ superconductor (SNS) junctions on nano wires²¹. However, no studies have ever tried to analyze features of Cooper pairs which support the anomalous transport properties. We address this issue in the present Letter.

Odd-frequency Cooper pairing was originally proposed to understand nature of unconventional superfluidity and superconductivity²². Ubiquitous appearance of the odd-frequency pairs at the surface of superconductors and near the interface of superconducting junctions has been established and widely accepted in recent years^{23,24}. The zero-energy Andreev bound state (ABS) at the surface of unconventional superconductors²⁶ is reinterpreted in terms of the odd-frequency Cooper pairing²⁵. In particular, the odd-frequency Cooper pairs make the background

of the anomalous proximity effect in a diffusive normal metal attached to a spin-triplet superconductor²⁷: (i) the large zero-energy quasiparticle density of states in a normal metal^{28,29}, (ii) the quantized zero-bias conductance at twice of the Sharvin's value in diffusive NS junctions²⁹, (iii) the fractional current(J)-phase(φ) relationship of $J \propto \sin(\varphi/2)$ in diffusive SNS junctions³⁰, (iv) the zero-bias anomaly in nonlocal conductance spectra³¹ and (v) the anomalous surface impedance in NS bilayers³².

In this Letter, we show that disordered NS and SNS junctions of nano wire indicate the properties of (i)-(iii) when the superconducting nano wire is topologically nontrivial. In addition, the amplitude of odd-frequency pairs in the normal nano wire suddenly grows as soon as the superconducting nano wire undergoes the transition to topologically nontrivial phase. The unusual transport phenomena due to the MFs²⁰ are nothing but the anomalous proximity effect due to the odd-frequency pairs. We will conclude that the odd-frequency Cooper pairs are indispensable to realizing MFs in solids.

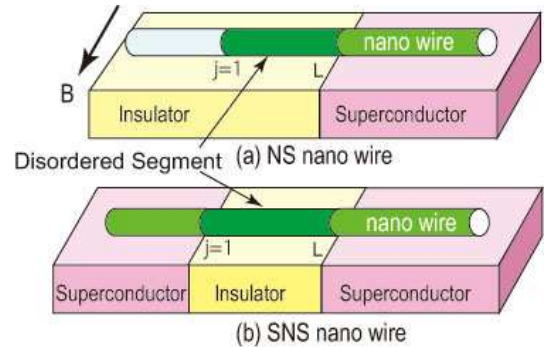


FIG. 1: (color online). Schematic pictures of NS and SNS junctions.

Let us consider a nano wire with strong spin-orbit coupling fabricated on a junction of an insulator and a metallic superconductor as shown in Fig. 1. A segment on the

insulator and that on the superconductor are in the normal and the superconducting states, respectively. The diameter of the nano wire is sufficiently small so that the number of propagating channel is unity for each spin degree of freedom. We describe the present nano wire by using the tight-binding model in one-dimension, for noninteracting electrons³³,

$$H_0 = -t \sum_{j,\alpha} \left(c_{j+1,\alpha}^\dagger c_{j,\alpha} + c_{j,\alpha}^\dagger c_{j+1,\alpha} \right) + i \frac{\lambda}{2} \sum_{j,\alpha,\beta} \left[c_{j+1,\alpha}^\dagger (\hat{\sigma}_2)_{\alpha,\beta} c_{j,\beta} - c_{j,\alpha}^\dagger (\hat{\sigma}_2)_{\alpha,\beta} c_{j+1,\beta} \right] + \sum_{j,\alpha,\beta} c_{j,\alpha}^\dagger \{ (2t - \mu) \hat{\sigma}_0 - V_{ex} \hat{\sigma}_3 \}_{\alpha,\beta} c_{j,\beta}, \quad (1)$$

$$H_s = \sum_{j \geq L+1} \left[\Delta e^{i\varphi} c_{j,\uparrow}^\dagger c_{j,\downarrow}^\dagger + \text{H.c.} \right], \quad (2)$$

$$H_d = \sum_{1 \leq j \leq L,\alpha} V_j c_{j,\alpha}^\dagger c_{j,\alpha}, \quad (3)$$

$$H_{s2} = \sum_{j \leq 0} \left[\Delta e^{i\varphi_2} c_{j,\uparrow}^\dagger c_{j,\downarrow}^\dagger + \text{H.c.} \right], \quad (4)$$

where $c_{j,\alpha}^\dagger$ ($c_{j,\alpha}$) is the creation (annihilation) operator of an electron at the lattice site j with spin $\alpha = (\uparrow \text{ or } \downarrow)$, t denotes the hopping integral, μ is the chemical potential, and Δ is the pair potential in the superconducting segment. The Pauli matrices in spin space are denoted by $\hat{\sigma}_j$ for $j = 1-3$ and the unit matrix of 2×2 is $\hat{\sigma}_0$. The on-site potential in the normal segment is given randomly in the range of $-W/2 \leq V_j \leq W/2$. We measure the energy and the length in units of t and the lattice constant, respectively. Throughout this paper, we fix several parameters as $\mu = t$, $W = 2t$, and the pair potential at the zero temperature $\Delta = 0.01t$. The number of samples used for the random ensemble averaging is typically $10^3 - 10^5$. By tuning the magnetic field B as shown in Fig. 1, it is possible to introduce external Zeeman potential V_{ex} . For $V_{ex} > V_c \equiv \sqrt{\Delta_0^2 + \mu^2}$, the number of propagating channels becomes unity and the superconducting segment undergoes the transition to topologically nontrivial phase. In the tight-binding model, the finite band width gives an additional condition $V_{ex} < V_{c2} \equiv 4t - \mu$ for the topological phase. Here we briefly summarize calculated results of the normal conductance of the disordered nano wires with using the recursive Green function method³⁴. By analyzing the Hamiltonian $H_0 + H_d$, we confirmed that the normal conductance decays exponentially with increasing L ³⁵. This is because one-dimensional disordered wires are basically in the localization regime.

At first, we calculate the differential conductance G_{NS} of NS junctions based on the standard formula³⁶,

$$G_{NS} = \frac{e^2}{h} \sum_{\alpha,\beta} \left[\delta_{\alpha,\beta} - |r_{\alpha,\beta}^{ee}|^2 + |r_{\alpha,\beta}^{he}|^2 \right]_{E=eV}, \quad (5)$$

where we consider the Hamiltonian $H_0 + H_d + H_s$. In Eq. (5), $r_{\alpha,\beta}^{ee}$ and $r_{\alpha,\beta}^{he}$ are the normal and Andreev re-

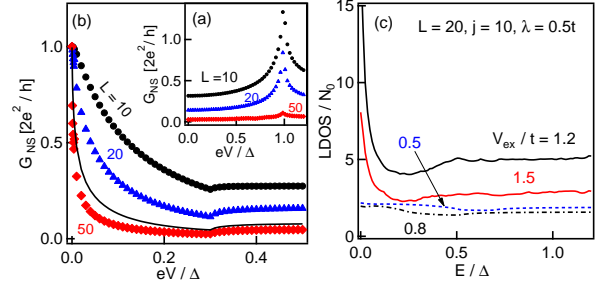


FIG. 2: (color online). The differential conductance of NS nano wires is plotted as a function of the bias-voltage for non-topological nano wire ($V_{ex} = \lambda = 0$) in (a) and for the topological nano wire ($V_{ex} = 1.5t$ and $\lambda = 0.5t$) in (b). In (b), we also plot the results for $W/t = 4$ and $L = 10$ with a solid line. The local density of states at the center of the disordered segment ($j = 10$) are shown for several V_{ex} in (c) with $\lambda = 0.5t$, where we add a small imaginary part $i\delta_\epsilon$ to the energy.

flexion coefficients of the junction at energy E measured from the fermi level. We show G_{NS} in units of $G_Q = 2e^2/h$ as a function of the bias-voltage eV for the non-topological and the topological nano wires in Figs. 2(a) and (b), respectively. The length of disordered segment L is chosen as 10, 20, and 50 lattice constants. The conductance for the non-topological nano wires ($V_{ex} = \lambda = 0$) in (a) decreases with increasing the length of disordered segment L for all eV . The similar tendency can be seen also in the conductance of the topological nano wires ($V_{ex} = 1.5t$ and $\lambda = 0.5t$) in (b) for finite eV . However the zero-bias conductance of the topological nano wires is quantized at G_Q irrespective of L , which is an intrinsic phenomenon in the presence of MF. The results suggest a perfect transmission channel due to the penetration of a resonant state into the disordered segment. The local density of states (LDOS) in the disordered nano wire supports this statement as shown in Fig. 2(c), where we plot the LDOS at the center of the disordered segment ($j = 10$) as a function of E for $L = 20$ and $\lambda = 0.5t$. The results are normalized to the density of states at the fermi level in clean normal nano wire N_0 . The LDOS for $V_{ex} > V_c$ show the large zero-energy peak reflecting the MBS as shown in the results for $V_{ex}/t = 1.5$ and 1.2 . On the other hand, the LDOS for $V_{ex}/t = 0.5$ and 0.8 are almost flat around the zero energy.

Secondly, we explain why the superconducting nano wire shows the anomalous proximity effect which is unique to the p_x -wave spin-triplet superconductor. The single particle Hamiltonian in Eq. (1) is essentially equivalent to $\hat{h}_0(k) = \xi_k \hat{\sigma}_0 - \lambda k \hat{\sigma}_2 - V_{ex} \hat{\sigma}_3$ in momentum space with $\xi_k = \hbar^2 k^2 / (2m) - \mu$. By applying a unitary transformation diagonalizing $h_0(k)$ and $-h_0^*(-k)$, Bogoliubov-de Gennes (BdG) Hamiltonian of the nanowire reduces to 2×2 Hamiltonian for $V_{ex} > V_c$ (See also Appendix A for

details),

$$\begin{bmatrix} \hat{h}_0(k) & i\Delta\hat{\sigma}_2 \\ -i\Delta^*\hat{\sigma}_2 & -\hat{h}_0^*(-k) \end{bmatrix} \rightarrow \begin{bmatrix} \xi_k - A & \tilde{\Delta}_k e^{i\pi/2} \\ \tilde{\Delta}_k e^{-i\pi/2} & -\xi_k + A \end{bmatrix}, \quad (6)$$

with $A = \sqrt{V_{ex}^2 + (\lambda k)^2}$ and $\tilde{\Delta}_k = \Delta \lambda k / A$ because a spin branch pinches off from the fermi level (i.e., $\xi + A > 0$). The right-hand side of Eq. (6) is equivalent to the BdG Hamiltonian of spin less p_x -wave superconductor in one-dimension when we focus on low energy excitation after redefining the chemical potential $\mu + A \rightarrow \mu$ and the pair potential $\tilde{\Delta}_k e^{i\pi/2} \rightarrow \Delta(k/k_F)$ with k_F being the fermi wave number. Therefore physics in the topological nanowire is the same as that of p_x -wave superconductor. In fact, we have confirmed that the Josephson current in SNS junctions of disordered nanowire show the fractional current-phase relationship at low temperature as shown in Fig. 3(a)³⁰. Here we attach the second superconductor for $j \leq 0$ by adding H_{s2} to $H_0 + H_s + H_d$, and plot the Josephson current J as a function of $\Delta\varphi = \varphi_2 - \varphi$ at $T = 0.001T_c$ for $V_{ex} = 1.5t$ and $\lambda = 0.5t$. The results show $J \propto \sin(\Delta\varphi/2)$ for $-\pi \leq \Delta\varphi \leq \pi$ irrespective of L . For comparison, we also plot the results for $V_{ex} = \lambda = 0$ and $L = 50$ with a solid line which shows usual sinusoidal current phase relationship. Correspondingly the Josephson critical current plotted as a function of temperature shows so called low temperature anomaly³⁰ in Fig. 3(b).

Next we discuss the relationship between Majorana fermions and odd-frequency Cooper pairs by analyzing the Green functions in junctions of p_x -wave superconductor. A semi-infinite wire of p_x -wave superconductor occupying $x > 0$ hosts a Majorana fermion around its edge at $E = 0$. Solving the BdG equation, the wave function of such surface state is calculated to be $\phi_0(x)^T = [u_0(x), v_0(x)]^T$, where $u_0(x) = C(x)\chi$, $v_0(x) = C(x)\chi^*$, $C(x) = \sqrt{2/\xi_0}e^{-x/2\xi_0} \sin(kx)$, $\chi = e^{i\pi/4}e^{i\varphi/2}$, and ξ_0 is the coherence length. The electron operator includes the contribution from such surface state $\psi_0(x)$ as represented by $\psi_0(x) = \chi\gamma(x)$, $\psi_0^\dagger(x) = \chi^*\gamma^\dagger(x)$ with $\gamma(x) = C(x)(\gamma_0 + \gamma_0^\dagger)$. Here γ_0 is the annihilation operator of the Majorana bound state. The special relation $v_0(x) = u_0^*(x)$ plays a crucial role in the Majorana relation of $\gamma(x) = \gamma^\dagger(x)$ ²⁵. As a result, the two Green functions calculated for $|E| \ll \Delta$

$$g(E; x, x') \approx \frac{u_0(x)u_0^*(x') + v_0^*(x)v_0(x')}{E + i\delta_\epsilon}, \quad (7)$$

$$f(E; x, x') \approx \frac{u_0(x)v_0^*(x') + v_0^*(x)u_0(x')}{E + i\delta_\epsilon}, \quad (8)$$

depend on each other. Since $v_0(x) = u_0^*(x)$, they satisfy

$$g(E, x, x') = (\chi^*)^2 f(E, x, x') = I(E; x, x'). \quad (9)$$

This relation directly bridges Majorana fermions and odd-frequency Cooper pairs. The real (imaginary) part of $(\chi^*)^2 f(E; x, x')$ is an odd (even) function of E , which

represents the odd-frequency symmetry of Cooper pairs. The orbital part is s -wave symmetry when f is calculated at $x = x'$. In fact, the imaginary part of $g(E; x, x')$ must be even function of E because it represents LDOS of the Majorana bound state. It is possible to check this argument in a junction which consists of a normal metal ($x < 0$) and a p_x -wave superconductor ($x > 0$) in one-dimension³⁸ (See also Appendix B). At the NS interface ($x = 0$), we introduce a potential barrier $V_0\delta(x)$ whose normal transmission coefficient is $t_n = k_F/(k_F + iz_0)$ with $z_0 = V_0/\hbar v_F$. When we focus on the subgap energy $|E| \ll \Delta$ in the tunneling limit $|t_n| \ll 1$, we find that the Green functions in the superconductor $x > 0$ satisfy Eq. (9) and become

$$I(E; x, x) \approx \frac{\pi N_0 \Delta}{E + i\Delta|t_n|^2/2} e^{-x/\xi_0} \sin^2(kx). \quad (10)$$

For comparison, we show the anomalous Green function in a uniform p_x -wave superconductor

$$(\chi^*)^2 f(E; x, x') = -i \frac{\pi N_0}{2} \frac{\Delta \sin k(x - x')}{\sqrt{(E + i0^+)^2 - \Delta^2}}, \quad (11)$$

with $\sqrt{(E + i0^+)^2 - \Delta^2}$ being $\text{sgn}(E)\sqrt{E^2 - \Delta^2}$ for $|E| > \Delta$ and $i\sqrt{\Delta^2 - E^2}$ for $|E| < \Delta$, where we assume $|x - x'| \ll \xi_0$. The anomalous Green function satisfies $f(x - x') = -f(x' - x)$ reflecting the odd-parity symmetry. In contrast to Eq. (10), the real (imaginary) part of $(\chi^*)^2 f(E, x, x')$ is an even (odd) function of E , which represents the even-frequency symmetry.

The important relation in Eq. (9) can be confirmed in the normal segment of NS nano wire as shown in Fig. 4, where we fix the energy at $E = 0$ and plot $g_{\uparrow\uparrow}(j, j)$ and $-f_{\uparrow\uparrow}(j, j)$ at the center of the normal segment $j = 10$. We note that an extra phase factor $\varphi = \pi/2$ in Eq. (6) makes $(\chi^*)^2 = -1$ in Eq. (9). For $V_{ex} > V_c$, the results show

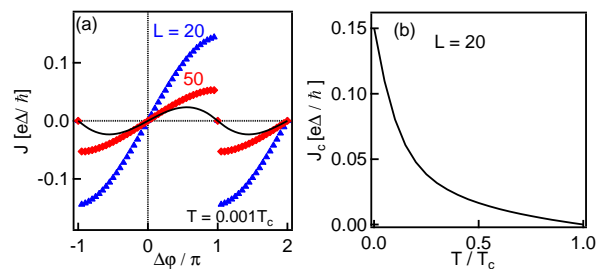


FIG. 3: (color online). (a): Current-phase relationship in SNS junctions of topological wire at $T/T_c = 0.001$ for $V_{ex} = 1.5t$ and $\lambda = 0.5t$. For comparison, the results for non topological wire ($V_{ex} = \lambda = 0$ and $L = 50$) is plotted with a solid line. (b): The Josephson critical current versus temperature in a topological nano wire.

$\text{Im}(g_{\uparrow\uparrow}) = -\text{Im}(f_{\uparrow\uparrow})$. The real part of $f_{\uparrow\uparrow}$ is always zero at $E = 0$ due to the odd-frequency symmetry. Correspondingly, $\text{Re}(g_{\uparrow\uparrow})$ also goes to zero for $V_{ex} > V_c$. In addition,

$-\text{Im}(g_{\uparrow\uparrow}) = \text{Im}(f_{\uparrow\uparrow})$ suddenly increases as V_{ex} increasing across V_C , which corresponds to the zero-energy peak in LDOS in Fig. 2(c). The results demonstrate the penetration of Majorana fermions and odd-frequency Cooper pairs into the normal disordered segment at the same time.

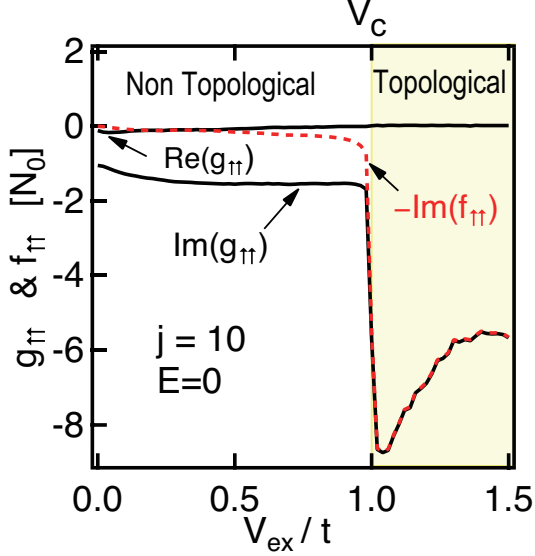


FIG. 4: (color online). The normal $g_{\uparrow\uparrow}$ and the anomalous $f_{\uparrow\uparrow}$ Green function for $E = 0$ at $j = 10$, with $L = 20$. We introduce a small imaginary part $\delta_\epsilon = 0.001\Delta$.

In the NS junction of p_x -wave superconductor, it is possible to calculate exactly the wave function in the presence of a single impurity $V_i\delta(x - x_i)$ in the normal metal by solving the Lippmann-Schwinger equation³⁸ (See also Appendix C),

$$\phi_n(x) = \phi_n^{ini}(x) + \hat{G}(E; x, x_i)V_i\hat{\sigma}_3\phi_n(x_i), \quad (12)$$

where $\phi_n(x)$ is the wave function in the presence of the impurity and $[\phi_n^{ini}(x)]^T = [e^{ikx} + r_{ee}e^{-ikx}, r_{he}e^{ikx}]^T$ is

that in the ballistic case with r_{ee} and r_{he} being the normal and the Andreev reflection coefficients at the NS interface from the electron branch, respectively. By putting $x = x_i$, the equation in Eq. (12) has the closed form for $\phi_n(x_i)$, which results in

$$\phi_n(x) = \phi_n^{ini}(x) + \frac{1}{Y} \begin{bmatrix} -e^{ikx}e^{2ikx_i}z_i(z_i + i)X \\ e^{ikx}(1 - Y)r_{he} \end{bmatrix}, \quad (13)$$

at $E = 0$ for $x < x_i$, where $Y = 1 + z_i^2X$, $X = 1 - r_{he}r_{eh}$, $z_i = V_i/\hbar v_F$, and r_{eh} is the Andreev reflection coefficient of the NS interface from the hole branch. We have already taken into account the absence of the normal reflection at the NS interface at $E = 0$ (i.e., $r_{ee} = r_{hh} = 0$). At $E = 0$, the Andreev reflection coefficients $r_{he} = -ie^{-i\varphi}$ and $r_{eh} = ie^{i\varphi}$ satisfy an important relation $r_{eh}r_{he} = 1$ which eliminates the second term of Eq. (13). Thus the zero-bias conductance quantization at $G_Q = 2e^2/h$ holds even in the presence of an impurity. The relation of $r_{eh}r_{he} = 1$ is nothing but the condition for forming the MBS at $E = 0$. To discuss whole effects of scatterings by many impurities, we need to solve the nonlinear quasi-classical Usadel equation^{28,29}. The analytical expression of the zero-bias conductance also show $G_{NS} = G_Q$ (See Appendix C). The diffusive normal metal is assumed in the Usadel equation. The validity of $G_{NS} = G_Q$ in the localization regime is confirmed in numerical calculation in Fig. 2(a) and in Fig. 6.

In summary, we have theoretically discussed the anomalous transport phenomena in NS and SNS junctions of nano wires in which the superconducting segment is topologically nontrivial and the normal segment is disordered by random impurity potential. The physics behind the anomalous transport can be understood in terms of the odd-frequency Cooper pairing. We conclude that Majorana fermions and odd-frequency Cooper pairs in solids are two sides of a same coin.

This work was supported by KAKENHI on Innovative Areas ‘‘Topological Quantum Phenomena’’ and KAKENHI(22540355,22103005) from MEXT of Japan.

Appendix A: Transformation of Hamiltonian

The starting Hamiltonian of this paper is equivalent to

$$H_{NW} = \begin{bmatrix} \hat{h}_k & i\Delta\hat{\sigma}_2e^{i\varphi} \\ -i\Delta\hat{\sigma}_2e^{-i\varphi} & -\hat{h}_{-k}^* \end{bmatrix}, \quad (A1)$$

$$h_k = \xi_k\hat{\sigma}_0 - V_{ex}\hat{\sigma}_3 - \lambda k\hat{\sigma}_2, \quad \xi_k = \frac{\hbar^2k^2}{2m} - \mu, \quad (A2)$$

where μ is the chemical potential, V_{ex} is the Zeeman potential due to external magnetic field, $\lambda k\hat{\sigma}_2$ represents the spin-orbit coupling, $\hat{\sigma}_0$ is the unit matrix in spin space, and $\hat{\sigma}_j$ for $j = 1 - 3$ are the Pauli’s matrices. By applying

following unitary transformation³⁹, the Hamiltonian is deformed as

$$\check{D}^\dagger H_{NW} \check{D} = \begin{bmatrix} \xi_k - A & 0 & \Delta_\lambda e^{i(\varphi+\pi/2)} & \Delta_V e^{i\varphi} \\ 0 & \xi_k + A & -\Delta_V e^{i\varphi} & \Delta_\lambda e^{i(\varphi-\pi/2)} \\ \Delta_\lambda e^{-i(\varphi+\pi/2)} & -\Delta_V e^{-i\varphi} & -\xi_k + A & 0 \\ \Delta_V e^{-i\varphi} & \Delta_\lambda e^{-i(\varphi-\pi/2)} & 0 & -\xi_k - A \end{bmatrix}, \quad (\text{A3})$$

$$\Delta_\lambda = \Delta \frac{\lambda k}{A}, \quad \Delta_V = \Delta \frac{V_{ex}}{A}, \quad A = \sqrt{V_{ex}^2 + (\lambda k)^2} \quad (\text{A4})$$

$$\check{D} = \begin{bmatrix} \hat{U} & 0 \\ 0 & \hat{U} \end{bmatrix}, \quad \hat{U} = \begin{bmatrix} \alpha & i \operatorname{sgn}(k)\beta \\ i \operatorname{sgn}(k)\beta & \alpha \end{bmatrix}, \quad (\text{A5})$$

$$\alpha = \sqrt{\frac{1}{2} \left(1 + \frac{V_{ex}}{A} \right)}, \quad \beta = \sqrt{\frac{1}{2} \left(1 - \frac{V_{ex}}{A} \right)}. \quad (\text{A6})$$

The topologically nontrivial phase is characterized by $V_{ex} > \sqrt{\mu^2 + \Delta^2}$. In such case, only one dispersion remains at the fermi level for each Nambu space (i.e., $\xi_k + A > 0$). Therefore the Hamiltonian reduces to 2×2 Nambu space as

$$\hat{H}_{NW2} = \begin{bmatrix} \xi_k - A & \Delta_\lambda e^{i(\varphi+\pi/2)} \\ \Delta_\lambda e^{-i(\varphi+\pi/2)} & -\xi_k + A \end{bmatrix}. \quad (\text{A7})$$

When we focus on the low-energy quasiparticle excitation, this is equivalent to the Hamiltonian describing the equal spin-triplet (spin less) p_x -wave superconductor

$$\hat{H}_{p_x} = \begin{bmatrix} \xi_k & \Delta \frac{k}{k_F} e^{i\varphi} \\ \Delta \frac{k}{k_F} e^{-i\varphi} & -\xi_k \end{bmatrix}. \quad (\text{A8})$$

Here we redefine $\mu + A \rightarrow \mu$ in the diagonal term and $\Delta_\lambda e^{i\pi/2} \rightarrow \Delta(k/k_F)$ in the off-diagonal term. In previous papers^{24,27,28,30-32}, we have studied the anomalous proximity effect starting from the Hamiltonian in Eq. (A8).

Appendix B: Analysis of p_x -wave superconductor

1. Green function and its representation

The retarded Green functions are defined by the standard way

$$\hat{G}(x, t; x', t') = -i\Theta(t - t') \begin{bmatrix} \{\psi(x, t), \psi^\dagger(x', t')\} & \{\psi(x, t), \psi(x', t')\} \\ \{\psi^\dagger(x, t), \psi^\dagger(x', t')\} & \{\psi^\dagger(x, t), \psi(x', t')\} \end{bmatrix}, \quad (\text{B1})$$

$$= \begin{bmatrix} G(x, t; x', t') & F(x, t; x', t') \\ \tilde{F}(x, t; x', t') & \tilde{G}(x, t; x', t') \end{bmatrix}, \quad (\text{B2})$$

where $\psi(x)(\psi^\dagger(x))$ is the annihilation (creation) operator of a spin less electron. In the case of spin-triplet superconductors, the electron operators are represented by the Bogoliubov transformation

$$\begin{bmatrix} \psi(x) \\ \psi^\dagger(x) \end{bmatrix} = \sum_\nu \begin{bmatrix} u_\nu(x) & v_\nu^*(x) \\ v_\nu(x) & u_\nu^*(x) \end{bmatrix} \begin{bmatrix} \gamma_\nu \\ \gamma_{-\nu}^\dagger \end{bmatrix}, \quad (\text{B3})$$

where γ_ν is the annihilation operators of Bogoliubov quasiparticle belonging to E_ν . The wave function $u_\nu(x)$ and $v_\nu(x)$ are obtained by solving the Bogoliubov-de Gennes (BdG) equation. The Green functions are expressed in spectral representation as

$$G(E; x, x') = \sum_\nu \left[\frac{u_\nu(x)u_\nu^*(x')}{E + i\delta - E_\nu} + \frac{v_\nu^*(x)v_\nu(x')}{E + i\delta + E_\nu} \right], \quad (\text{B4})$$

$$F(E; x, x') = \sum_\nu \left[\frac{u_\nu(x)v_\nu^*(x')}{E + i\delta - E_\nu} + \frac{v_\nu^*(x)u_\nu(x')}{E + i\delta + E_\nu} \right], \quad (\text{B5})$$

where $i\delta$ is a small imaginary part.

2. Uniform superconductor

The retarded Green function of a uniform spin less p_x -wave superconductor is calculated to be

$$\hat{G}(E; x, x') = \frac{-i\pi N_0}{2\Omega} \hat{\Phi} \left[\begin{pmatrix} E + \Omega & \Delta s_x \\ \Delta s_x & E - \Omega \end{pmatrix} e^{ik^+|x-x'|} + \begin{pmatrix} E - \Omega & -\Delta s_x \\ -\Delta s_x & E + \Omega \end{pmatrix} e^{-ik^-|x-x'|} \right] \hat{\Phi}^*, \quad (\text{B6})$$

$$\hat{G}(E; x, x') = \begin{pmatrix} G(E; x, x') & F(E; x, x') \\ \tilde{F}(E; x, x') & \tilde{G}(E; x, x') \end{pmatrix}, \quad (\text{B7})$$

$$k^\pm = k \left(1 \pm \frac{\Omega}{2\mu} \right), \quad \Omega = \sqrt{(E + i\delta)^2 - \Delta^2}, \quad \hat{\Phi} = \text{diag}[e^{i\varphi/2}, e^{-i\varphi/2}], \quad s_x = \text{sgn}(x - x'), \quad (\text{B8})$$

where N_0 is the density of states (DOS) at the fermi level in the normal state. The Green functions are calculated as

$$G(E; x, x') = -i \frac{\pi N_0}{2} e^{ik\Omega|x-x'|/(2\mu)} \left[\frac{E}{\Omega} \cos k(x-x') + i \sin k|x-x'| \right], \quad (\text{B9})$$

$$-ie^{-i\varphi} F(E; x, x') = -i \frac{\pi N_0}{2} e^{ik\Omega|x-x'|/(2\mu)} \frac{\Delta}{\Omega} \sin k(x-x'). \quad (\text{B10})$$

From the normal Green functions, the local density of states (LDOS) is calculated to be

$$N(E, x) = \frac{-1}{\pi} \text{ImTr} \hat{G}(E, x, x) = N_0 \text{Re} \frac{E}{\Omega}. \quad (\text{B11})$$

The LDOS is an even function of E because of the relation

$$\sqrt{(E + i\delta)^2 - \Delta^2} = \begin{cases} \sqrt{E^2 - \Delta^2} & \Delta < E \\ i\sqrt{\Delta^2 - E^2} & 0 < |E| < \Delta \\ -\sqrt{E^2 - \Delta^2} & E < -\Delta \end{cases}. \quad (\text{B12})$$

It is evident that there is no subgap state in uniform superconductor. From the off-diagonal part, it is possible to check the pairing symmetry. The anomalous Green function satisfies $F(x-x') = -F(x'-x)$, which indicates the odd-parity symmetry. In addition, the real part of $-ie^{-i\varphi} F(E, x, x')$ is an even function of E , whereas the imaginary part of it is an odd function of E . This means that Cooper pairs have the even-frequency symmetry.

3. Majorana surface bound state

Next we consider a semi-finite p_x -wave superconductor which occupies $x > 0$ as shown in Fig. 1(a). By solving the Bogoliubov-de Gennes equation, the wave function for subgap state is expressed by

$$\Psi_S(x) = A \begin{bmatrix} E + i\tilde{\Omega} \\ \Delta e^{-i\varphi} \end{bmatrix} e^{ikx} e^{-x/2\xi_0} + B \begin{bmatrix} E - i\tilde{\Omega} \\ -\Delta e^{-i\varphi} \end{bmatrix} e^{-ikx} e^{-x/2\xi_0}, \quad (\text{B13})$$

where $\tilde{\Omega} = \sqrt{\Delta^2 - E^2}$, A and B are constant. From the boundary condition at $x = 0$ (i.e., $\Psi_S(x=0) = 0$), we find that a subgap state exists at $E = 0$ and that the wave function of it becomes

$$\Psi_S(x) = \begin{bmatrix} u_0(x) \\ v_0(x) \end{bmatrix} = C(x) \begin{bmatrix} e^{i\pi/4} e^{i\varphi/2} \\ e^{-i\pi/4} e^{-i\varphi/2} \end{bmatrix}, \quad C(x) = \sqrt{\frac{2}{\xi_0}} e^{-x/2\xi_0} \sin(kx). \quad (\text{B14})$$

We note that two components in the wave function satisfy an important relation

$$u_0(x) = v_0^*(x). \quad (\text{B15})$$

The BdG transformation reads,

$$\begin{bmatrix} \psi(x) \\ \psi^\dagger(x) \end{bmatrix} = \sum_{\nu \neq 0} \begin{bmatrix} u_\nu(x) & v_\nu^*(x) \\ v_\nu(x) & u_\nu^*(x) \end{bmatrix} \begin{bmatrix} \gamma_\nu \\ \gamma_{-\nu}^\dagger \end{bmatrix} + \begin{bmatrix} \phi_0(x) \\ \phi_0^\dagger(x) \end{bmatrix}, \quad (\text{B16})$$

$$\begin{bmatrix} \phi_0(x) \\ \phi_0^\dagger(x) \end{bmatrix} = \begin{bmatrix} u_0(x) & v_0^*(x) \\ v_0(x) & u_0^*(x) \end{bmatrix} \begin{bmatrix} \gamma_0 \\ \gamma_0^\dagger \end{bmatrix}, \quad (\text{B17})$$

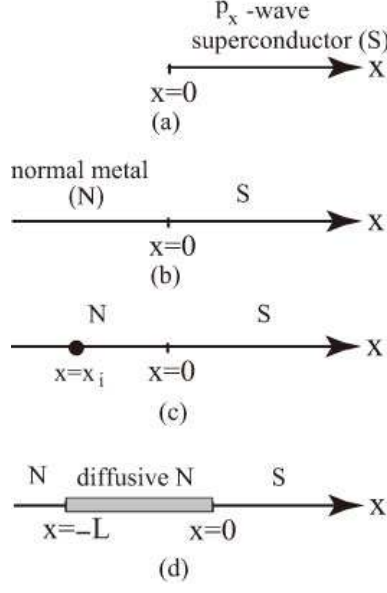


FIG. 5: System under consideration. (a): a semi-infinite p_x -wave superconductor. (b): a clean normal-metal/superconductor (NS) junction of p_x -wave symmetry. (c): an impurity is introduced in the normal metal. (d): a diffusive normal metal is introduced in the NS junction.

where γ_0 is the annihilation operator of the bound state. Together with Eqs. (B14) and (B15), we find

$$\phi_0(x) = e^{i\pi/4} e^{i\varphi/2} \gamma(x), \quad \phi_0^\dagger(x) = e^{-i\pi/4} e^{-i\varphi/2} \gamma(x), \quad (\text{B18})$$

$$\gamma(x) = C(x)(\gamma_0 + \gamma_0^\dagger). \quad (\text{B19})$$

The fermion operator $\gamma(x)$ satisfies the Majorana relation $\gamma(x) = \gamma^\dagger(x)$. When we focus on $|E| \ll \Delta$, the contributions from $\nu = 0$ become dominant in Eqs. (B4) and (B5). Near $E = 0$, the normal and the anomalous Green functions satisfy a relation

$$G(E; x, x') = -ie^{-i\varphi} F(E; x, x'), \quad (\text{B20})$$

because they are calculated from Eq. (B17) as

$$G(E; x, x') = \frac{2C(x)C(x')}{E + i\delta}, \quad F(E; x, x') = \frac{2C(x)C(x')}{E + i\delta} ie^{i\varphi}. \quad (\text{B21})$$

Eq. (B20) directly relates Majorana fermions and odd-frequency Cooper pairs. When we consider $x = x'$, $F(E, x, x)$ represents the pairing function of s -wave symmetry. The real part of $-ie^{-i\varphi} F(E; x, x)$ is an odd-function of E and the imaginary part of it is an even function of E . This indicates that Cooper pairs have the odd-frequency symmetry. It is possible to confirm Eq. (B20) in NS junctions as discussed below.

4. NS junction of p_x superconductor

It is possible to calculate the Green function of a junction which consists of a normal metal ($x < 0$) and a p_x -wave superconductor ($x > 0$) in one dimension as shown in Fig. 1(b). In the superconductor, the retarded Green function

becomes³⁸

$$\begin{aligned} \hat{G}_{ss}(E; x, x') &= \hat{\Phi} i \frac{N_0 \pi E}{2 \Omega} \\ &\times \left[\begin{pmatrix} u^2 & uvs_x \\ uvs_x & v^2 \end{pmatrix} e^{ik^+|x-x'|} + \begin{pmatrix} v^2 & -uvs_x \\ -uvs_x & u^2 \end{pmatrix} e^{-ik^-|x-x'|} \right. \\ &+ \begin{pmatrix} -uv & v^2 \\ u^2 & -uv \end{pmatrix} e^{-ik^-x+ik^+x'} r_{ss}^{he} + \begin{pmatrix} uv & u^2 \\ v^2 & uv \end{pmatrix} e^{ik^+x-ik^-x'} r_{ss}^{eh} \\ &\left. + \begin{pmatrix} u^2 & -uv \\ uv & -v^2 \end{pmatrix} e^{ik^+(x+x')} r_{ss}^{ee} + \begin{pmatrix} -v^2 & -uv \\ uv & u^2 \end{pmatrix} e^{-ik^-(x+x')} r_{ss}^{hh} \right] \hat{\Phi}^*, \end{aligned} \quad (\text{B22})$$

$$\hat{G}_{ss}(E; x, x') = \begin{pmatrix} G_{ss}(E; x, x') & F_{ss}(E; x, x') \\ \tilde{F}_{ss}(E; x, x') & \tilde{G}_{ss}(E; x, x') \end{pmatrix}, \quad \hat{\Phi} = \text{diag}(e^{i\varphi/2}, e^{-i\varphi/2}), \quad (\text{B23})$$

$$u(v) = \sqrt{\frac{1}{2} \left(1 + (-) \frac{\Omega}{E} \right)}, \quad \Omega = \sqrt{(E + i\delta)^2 - \Delta^2}, \quad k^\pm = k \left(1 \pm \frac{\Omega}{2\mu} \right), \quad s_x = \text{sgn}(x - x') \quad (\text{B24})$$

for $x, x' > 0$. The subscript ss in the Green function $\hat{G}_{ss}(E; x, x')$ means that both $x > 0$ and $x' > 0$ indicate places in the superconductor. The normal and Andreev reflection coefficients are given by

$$r_{ss}^{he} = \frac{uv}{\Xi} (2 - |t_n|^2) = -r_{ss}^{eh}, \quad r_{ss}^{ee} = \frac{r}{\Xi} (u^2 - v^2), \quad r_{ss}^{hh} = \frac{r^*}{\Xi} (u^2 - v^2), \quad (\text{B25})$$

$$\Xi = 1 - |t_n|^2 v^2, \quad t_n = \frac{k}{k + iz_0}, \quad r_n = \frac{-iz_0}{k + iz_0}, \quad z_0 = V_0 / \hbar v_F \quad (\text{B26})$$

where t_n and r_n are the normal transmission coefficients due to the potential barrier at the interface described by $V_0 \delta(x)$. When we focus on the subgap energy in the tunneling limit (i.e., $|E| \ll \Delta$ and $|t_n| \ll 1$), we find,

$$G_{ss}(E; x, x) = -ie^{-i\varphi} F_{ss}(E; x, x) \approx \pi N_0 \frac{\Delta}{E + i\Delta |t_n|^2 / 2} e^{-x/\xi_0} \sin^2(kx). \quad (\text{B27})$$

The imaginary part of $G_{ss}(E; x, x)$ gives the local density of the Andreev bound state and must be an even function of E . Therefore the real part of $-ie^{-i\varphi} F_{ss}(E; x, x)$ is an odd-function of E and the imaginary part of it is an even function of E , which indicates the odd-frequency symmetry. The condition in Eq. (B15) leads to the Majorana relation in operators at Eq. (B18). Eq. (B18) results in Eq. (B20). Then Eq. (B20) guarantees the odd-frequency symmetry of Cooper pairs. The orbital part of Cooper pairs is s -wave symmetry because $-ie^{-i\varphi} F_{ss}$ is calculated at $x = x'$.

Appendix C: Perfect transmission at $E = 0$

In the normal metal of NS junction ($x, x' < 0$), the Green function is given by³⁸

$$\hat{G}_{nn}(E; x, x') = -i \frac{\pi N_0}{2} \begin{bmatrix} e^{-ik|x-x'|} + e^{-ik(x+x')} r_{nn}^{ee} & e^{-ikx+ikx'} r_{nn}^{eh} \\ e^{ikx-ikx'} r_{nn}^{he} & e^{ik|x-x'|} + e^{ik(x+x')} r_{nn}^{hh} \end{bmatrix}, \quad (\text{C1})$$

$$r_{nn}^{he} = \frac{|t_n|^2 e^{-i\varphi} uv}{\Xi}, \quad r_{nn}^{eh} = -\frac{|t_n|^2 e^{i\varphi} uv}{\Xi}, \quad r_{nn}^{ee} = \frac{r_n}{\Xi}, \quad r_{nn}^{hh} = \frac{r_n^*}{\Xi}, \quad (\text{C2})$$

$$\hat{G}_{nn}(E; x, x') = \begin{pmatrix} G_{nn}(E; x, x') & F_{nn}(E; x, x') \\ \tilde{F}_{nn}(E; x, x') & \tilde{G}_{nn}(E; x, x') \end{pmatrix}. \quad (\text{C3})$$

$$(\text{C4})$$

The subscript nn in the Green function $\hat{G}_{nn}(E; x, x')$ means that both $x < 0$ and $x' < 0$ indicate places in the normal metal. We also confirmed the relation between the Green function in the normal metal,

$$G_{nn}(E; x, x) = -ie^{-i\varphi} F_{nn}(E; x, x) \approx \pi N_0 \frac{\Delta |t_n|^2}{E + i\Delta |t_n|^2 / 2}, \quad (\text{C5})$$

for $|E| \ll \Delta$ and $|t_n|^2 \ll 1$. As we discussed in Eq. (B20), this suggests the presence of Majorana fermions and odd-frequency Cooper pairs in the normal metal.

It is possible to calculate exactly the wave function where a single impurity $V_i\delta(x-x_i)$ exist in the normal metal as shown in Fig. 1(c) by using the Lippmann-Schwinger equation,

$$\phi_n(x) = \phi_n^{ini}(x) + \hat{G}_{nn}(E; x, x_i)V_i\hat{\sigma}_3\phi_n(x_i), \quad (C6)$$

$$\phi_n^{ini}(x) = \begin{bmatrix} e^{ikx} + e^{-ikx}r_{nn}^{ee} \\ e^{ikx}r_{nn}^{he} \end{bmatrix} \quad (C7)$$

where $\phi_n^{ini}(x)$ is the wave function in the ballistic case and $\phi_n(x)$ is that in the presence of the impurity. By solving this equation at $x = x_i$, we obtain

$$\phi_n(x_i) = \left[1 - \hat{G}_{nn}(E; x_i, x_i)V_i\hat{\sigma}_3\right]^{-1} \phi_n^{ini}(x_i). \quad (C8)$$

The wave function for $x < x_i$ in the presence of the single impurity is expressed by

$$\phi_n(x) = \phi_n^{ini}(x) + \hat{G}_{nn}(E; x, x_i)V_i\hat{\sigma}_3 \left[1 - \hat{G}_{nn}(E; x_i, x_i)V_i\hat{\sigma}_3\right]^{-1} \phi_n^{ini}(x_i), \quad (C9)$$

$$= \phi_n^{ini}(x) + \frac{1}{Y} \begin{bmatrix} e^{-ikx} \left\{ -iz_i(B_1^2 - e^{2ikx_i}r_{nn}^{he}r_{nn}^{eh}) - z_i^2 \{B_1B_2 - r_{nn}^{he}r_{nn}^{eh}\} e^{ikx_i}B_1 \right\} \\ e^{ikx}(1-Y)r_{nn}^{he} \end{bmatrix}, \quad (C10)$$

$$Y = 1 + z_i(e^{i2kx_i}r_{nn}^{hh} - e^{-i2kx_i}r_{nn}^{ee}) + z_i^2(1 - r_{nn}^{he}r_{nn}^{eh} + e^{i2kx_i}r_{nn}^{hh} + e^{-i2kx_i}r_{nn}^{ee}), \quad (C11)$$

$$B_1 = e^{ikx_i} + e^{-ikx_i}r_{nn}^{ee}, \quad B_2 = e^{-ikx_i} + e^{ikx_i}r_{nn}^{hh}, \quad z_i = V_i/\hbar v. \quad (C12)$$

At $E = 0$, the reflection coefficients become

$$r_{nn}^{eh} = ie^{i\varphi}, \quad r_{nn}^{he} = -ie^{-i\varphi}, \quad r_{nn}^{ee} = r_{nn}^{hh} = 0. \quad (C13)$$

These relations immediately lead to

$$B_1^2 - e^{2ikx_i}r_{nn}^{he}r_{nn}^{eh} = B_1B_2 - r_{nn}^{he}r_{nn}^{eh} = 0, \quad Y = 1. \quad (C14)$$

Therefore we find that the wave function in the presence of the single impurity at $x = x_i$ remains unchanged from the original one

$$\phi_n(x) = \begin{bmatrix} e^{ikx} \\ 0 \end{bmatrix} + \begin{bmatrix} 0 \\ -ie^{-i\varphi}e^{ikx} \end{bmatrix}. \quad (C15)$$

The first term represents the incoming wave at the electron branch. The second term expresses the outgoing wave in the hole branch. The Andreev reflection is perfect and the normal reflection is absent even in the presence of the single impurity in the normal metal. With using the Blonder-Tinkham-Klapwijk formula,

$$G_{NS} = \frac{e^2}{h} [1 - |r_{nn}^{ee}|^2 + |r_{nn}^{he}|^2], \quad (C16)$$

the zero-bias conductance of the NS junction remains unchanged from $G_{NS} = 2e^2/h$ independent of the impurity scattering.

On the way to the conclusion, we derive a relation

$$r_{nn}^{eh}r_{nn}^{he} = 1, \quad (C17)$$

at $E = 0$. This plays an important role in the resonant transmission of a quasiparticle in a normal metal. For comparison, the Andreev reflection coefficients of the s -wave transparent NS junction becomes

$$r_{nn}^{he} = -ie^{-i\varphi}, \quad r_{nn}^{eh} = -ie^{i\varphi}, \quad (C18)$$

at $E = 0$. However, they gives a relation $r_{nn}^{eh}r_{nn}^{he} = -1$. In this case, a quasiparticle is scattered by the impurity and the conductance decreases from $G_{NS} = G_Q$. The relation in Eq. (C17) is equivalent to the necessary condition for the formation of Andreev (Majorana) bound states at $E = 0$.

Appendix D: Analysis of quasiclassical Usadel Equation

In this section, we consider a diffusive normal metal is attached to p_x -wave superconductor as shown in Fig. 1(d). At first, we define the quasiclassical Green functions in terms of Gor'kov Green functions. In the mixed representation, Gor'kov Green functions become

$$G(x, t; x', t') = G(x_c, x - x', t_c, t - t') = \int \frac{d\epsilon}{2\pi} \int \frac{dk}{2\pi} G(x_c, k, t_c, \epsilon) e^{ik(x-x') - i\epsilon(t-t')}, \quad (\text{D1})$$

$$F(x, t; x', t') = F(x_c, x - x', t_c, t - t') = \int \frac{d\epsilon}{2\pi} \int \frac{dk}{2\pi} F(x_c, k, t_c, \epsilon) e^{ik(x-x') - i\epsilon(t-t')}, \quad (\text{D2})$$

$$x_c = \frac{x + x'}{2}, \quad t_c = \frac{t + t'}{2}. \quad (\text{D3})$$

When we consider static state, the Green functions are independent of t_c . With replacing x_c by x , the quasiclassical Green functions are defined as

$$g(x, k, \epsilon) = \frac{i}{\pi} \int d\xi_k G(x, k, \epsilon) - \frac{i}{\pi} \int d\xi_k \frac{\mathcal{P}}{\xi_k}, \quad (\text{D4})$$

$$f(x, k, \epsilon) = \frac{i}{\pi} \int d\xi_k F(x, k, \epsilon). \quad (\text{D5})$$

They obey so called Eilenberger equation. In what follows, we fix the phase of the superconductor φ at 0. When the normal metal is in the dirty limit, $g(x, k, \epsilon)$ and $f(x, k, \epsilon)$ are isotropic in momentum space. Since they satisfy the normalization condition $g^2(x, \epsilon) + f^2(x, \epsilon) = 1$, it is possible to apply a parameterization: $g(x, \epsilon) = \cos[\theta(x, \epsilon)]$ and $f(x, \epsilon) = \sin[\theta(x, \epsilon)]$. The function $\theta(x, \epsilon)$ obeys the Usadel equation in the diffusive normal metal

$$D \frac{\partial^2 \theta(x, \epsilon)}{\partial x^2} + 2i\epsilon \sin[\theta(x, \epsilon)] = 0, \quad (\text{D6})$$

where D is the diffusion constant in the dirty normal metal.

In what follows, we consider NS junction shown in Fig. 1(d), where a dirty normal metal is introduced between a clean normal lead wire ($x < -L$) and a p_x -wave superconductor ($x > 0$). The boundary condition for $\theta(x, \epsilon)$ are given by²⁸

$$\theta(x = -L, \epsilon) = 0, \quad (\text{D7})$$

$$\frac{L}{R_N} \frac{\partial \theta(x, \epsilon)}{\partial x} \Big|_{x=0} = \frac{2}{R_B} \frac{f_S \cos \theta_0 - g_S \sin \theta_0}{2 - |t_n|^2 + |t_n|^2 (f_S \sin \theta_0 + g_S \cos \theta_0)}, \quad (\text{D8})$$

with

$$\theta_0 = \theta(x = 0, \epsilon), \quad g_S = \frac{g_+ + g_-}{1 + g_+ g_- + f_+ f_-}, \quad f_S = i \frac{f_+ g_- - f_- g_+}{1 + g_+ g_- + f_+ f_-}, \quad (\text{D9})$$

$$R_B = [G_Q |t_n|^2]^{-1}, \quad G_Q = \frac{2e^2}{h}. \quad (\text{D10})$$

The parameter R_N and R_B are the normal resistance of the dirty normal metal and that due to the potential barrier at the NS interface, respectively. The information of the pairing symmetry of superconductor is embedded in the surface Green function g_S and f_S . The total resistance of the junction R is represented by²⁸

$$R = \tilde{R}_B + \tilde{R}_N, \quad (\text{D11})$$

$$\tilde{R}_B = \frac{1}{2} \frac{C_0}{|(2 - |t_n|^2) + |t_n|^2 (\cos \theta_0 g_S + \sin \theta_0 f_S)|^2}, \quad (\text{D12})$$

$$C_0 = |t_n|^2 (1 + |\cos \theta_0|^2 + |\sin \theta_0|^2) (1 + |g_S|^2 + |f_S|^2) + 4(2 - |t_n|^2) [\text{Re}(g_S) \text{Re}(\cos \theta_0) + \text{Re}(f_S) \text{Re}(\sin \theta_0)] + 4|t_n|^2 \text{Im}(\cos \theta_0 \sin^* \theta_0) \text{Im}(g_S^* f_S), \quad (\text{D13})$$

$$\tilde{R}_N = \frac{R_N}{L} \int_{-L}^0 \frac{2dx}{1 + |\cos \theta(x, \epsilon)|^2 + |\sin \theta(x, \epsilon)|^2}. \quad (\text{D14})$$

The resistance \tilde{R}_B and \tilde{R}_N are not equal to their normal one's R_B and R_N . They are modified by the proximity effect.

In the case of the p_x -wave superconductor, following relations hold

$$g_+ = g_- = \frac{\epsilon}{\sqrt{(\epsilon + i0^+)^2 - \Delta^2}}, \quad f_+ = -f_- = \frac{i\Delta}{\sqrt{(\epsilon + i0^+)^2 - \Delta^2}}. \quad (\text{D15})$$

The p_x -wave symmetry of superconductor is represented by the relation $f_+ = -f_-$. At the surface of p_x -wave superconductor, purely odd-frequency pairing state exist due to the formation of Andreev bound state as discussed in Sec. 2.3.

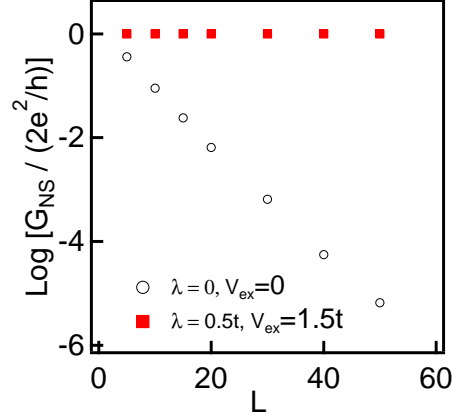


FIG. 6: Conductance are plotted as a function of L in NS junctions of nano wire.

The Usadel equation can be solved analytically at $\epsilon = 0$. Under the boundary condition $(L/R_N)(\partial\theta/\partial x)|_{x=0} = iG_Q$, we obtain

$$\theta(x, \epsilon = 0) = iR_N G_Q \frac{x+L}{L}, \quad (\text{D16})$$

$$g(x) = \cos \theta(x, 0) = \cosh \left(R_N G_Q \frac{x+L}{L} \right), \quad (\text{D17})$$

$$f(x) = \sin \theta(x, 0) = i \sinh \left(R_N G_Q \frac{x+L}{L} \right), \quad (\text{D18})$$

at $\epsilon = 0$. The pairing function $f(x)$ represents the spin-triplet s -wave odd-frequency pair. Indeed, $f(x)$ is purely imaginary number at $\epsilon = 0$. Finally we obtain the zero-bias resistance

$$R = \tilde{R}_B + \tilde{R}_N = G_Q^{-1}, \quad (\text{D19})$$

$$\tilde{R}_B = \frac{1}{G_Q} [1 + if(0)/g(0)] = \frac{1}{G_Q} [1 - \tanh(G_Q R_N)], \quad (\text{D20})$$

$$\tilde{R}_N = \frac{1}{G_Q} [-if(0)/g(0)] = \frac{1}{G_Q} \tanh(G_Q R_N). \quad (\text{D21})$$

The total resistance at the zero-bias voltage is independent of R_N and R_B , and remains unchanged from $R = G_Q^{-1}$. It is worth to consider the physical meaning of the resulting resistances \tilde{R}_B and \tilde{R}_N . \tilde{R}_B is the resistance at the interface which decreases from G_Q^{-1} with the increase of R_N . In other words, the interface resistance decreases with the increase of the amplitude of odd-frequency pair $f(0)$. \tilde{R}_N is the resistance of the dirty normal metal. In the limit of weak proximity effect $R_N G_Q \ll 1$, the amplitude of odd-frequency pairs becomes small. In such limit, we find $\tilde{R}_N = R_N$. On the other hand for $R_N G_Q \gg 1$, $-if(0)/g(0)$ goes to unity and \tilde{R}_N approaches to G_Q^{-1} . Thus the odd-frequency pairs play a crucial role in the relation of $R = G_Q^{-1}$.

The diffusive transport is assumed in the Usadel equation. It is possible to check the validity of $G_{NS} = G_Q$ when the normal segment is in the localization regime. In Fig. 6, we plot the zero-bias conductance in NS junctions of nano wire as a function of the length of the disordered segment L . When the nano wire is non topological at $\lambda = V_{ex} = 0$,

the zero-bias conductance decreases exponentially with L due to the localization. On the other hand, the conductance for topological nano wire junctions at $\lambda = 0.5t$ and $V_{ex} = 1.5t$ remains unchanged from G_Q even in the localization regime.

-
- ¹ E. Majorana, *Nuovo Cimento* **14**, 171 (1937).
- ² F. Wilczek, *Nat. Phys.* **5**, 614 (2009); M. Franz, *Physics* **3**, 24 (2010); J. Alicea, *Rep. Prog. Phys.* **75**, 076501 (2012).
- ³ D. A. Ivanov, *Phys. Rev. Lett.* **86**, 268 (2001).
- ⁴ S. Das Sarma, M. Freedman, and C. Nayak, *Phys. Rev. Lett.* **94**, 166802 (2005); C. Nayak et al., *Rev. Mod. Phys.* **80**, 1083 (2008).
- ⁵ N. Read and D. Green, *Phys. Rev. B* **61**, 10267 (2000).
- ⁶ C. J. Bolech and E. Demler, *Phys. Rev. Lett.*, **98**, 237002 (2007).
- ⁷ K. Sengupta, I. Zutic, H.-J. Kwon, V. M. Yakovenko, S. Das Sarma, *Phys. Rev. B* **63**, 144531 (2001).
- ⁸ A. Y. Kitaev, *Physics-Uspekhi* **44**, 131 (2001).
- ⁹ L. Fu and C. L. Kane, *Phys. Rev. Lett.* **100**, 096407 (2008).
- ¹⁰ M. Sato, Y. Takahashi, S. Fujimoto, *Phys. Rev. Lett.* **103**, 020401 (2009).
- ¹¹ J. D. Sau, R. M. Lutchyn, S. Tewari, and S. Das Sarma, *Phys. Rev. Lett.* **104**, 040502 (2010).
- ¹² J. Alicea, *Phys. Rev. B* **81**, 125318 (2010).
- ¹³ A. C. Potter and P. A. Lee, *Phys. Rev. Lett.* **105**, 227003 (2010); J. Linder and A. Sudbo, *Phys. Rev. B* **82**, 085314 (2010).
- ¹⁴ M. Sato and S. Fujimoto, *Phys. Rev. B* **79**, 094504 (2009); Y. Tanaka, T. Yokoyama, A. V. Balatsky, and N. Nagaosa, *Phys. Rev. B* **79**, 060505 (2009).
- ¹⁵ S. Sasaki, M. Kriener, K. Segawa, K. Yada, Y. Tanaka, M. Sato, and Y. Ando, *Phys. Rev. Lett.* **107**, 217001 (2011); L. Fu and E. Berg, *Phys. Rev. Lett.* **105**, 097001 (2010); T. H. Hsieh and L. Fu, *Phys. Rev. Lett.* **108**, 107005 (2012).
- ¹⁶ R. M. Lutchyn, J. D. Sau, and S. Das Sarma, *Phys. Rev. Lett.* **105**, 077001 (2010); J. D. Sau, S. Tewari, R. M. Lutchyn, T. D. Stanescu, and S. Das Sarma, *Phys. Rev. B* **82**, 214509 (2010).
- ¹⁷ Y. Oreg, G. Refael, and F. von Oppen, *Phys. Rev. Lett.* **105**, 177002 (2010).
- ¹⁸ S. Tewari, T. D. Stanescu, J. D. Sau, and S. Das Sarma, *New Journal of Physics* **13**, 065004 (2011). T. D. Stanescu, R. M. Lutchyn, and S. Das Sarma, *Phys. Rev. B* **84**, 144522 (2011); R. M. Lutchyn, T. D. Stanescu, and S. Das Sarma, *Phys. Rev. Lett.* **106**, 127001 (2011); R. M. Lutchyn and M. P. A. Fisher, *Phys. Rev. B* **84**, 214528 (2011).
- ¹⁹ A. Golub, I. Kuzmenko, and Y. Avishai, *Phys. Rev. Lett.* **107**, 176802 (2011); K. Flensberg, *Phys. Rev. B* **82**, 180516 (2010); A. Romito, J. Alicea, G. Refael, and F. von Oppen, *Phys. Rev. B* **85**, 020502 (2012); C. Bena, D. Sticlet, and P. Simon, *Phys. Rev. Lett.* **108**, 096802 (2012); A. C. Potter and P. A. Lee, *Phys. Rev. B*, **83**, 094525 (2011); B. Zhou and S.-Q. Shen, *Phys. Rev. B*, **84**, 054532 (2011); K. T. Law and P. A. Lee, *Phys. Rev. B*, **84**, 081304 (2011); J. Klinovaja and D. Loss, *Phys. Rev. B* **86**, 085408 (2012).
- ²⁰ V. Mourik, K. Zuo, S. M. Frolov, S. R. Plissard, E. P. A. M. Bakkers, and L. P. Kouwenhoven, *Science* **336**, 1003 (2012); A. Das, Y. Ronen, Y. Most, Y. Oreg, M. Heiblum, H. Shtrikman, *Nature Phys.* **8**, 887 (2012); L. P. Rokhinson, X. Liu, J. K. Furdyna, *Nature Phys.* **8**, 795 (2012); M. T. Deng, C. L. Yu, G. Y. Huang, M. Larsson, P. Caroff, H. Q. Xu, *Nano Letters* **12** 6414 (2012).
- ²¹ A. R. Akhmerov, J. P. Dahlhaus, F. Hassler, M. Wimmer, and C. W. J. Beenakker, *Phys. Rev. Lett.*, **106**, 057001 (2011); P. W. Brouwer, M. Duckheim, A. Romito, and F. von Oppen, *Phys. Rev. B*, **84**, 144526 (2011); C. Qu, Y. Zhang, L. Mao, and C. Zhang, arXiv:1109.4108; M. Gibertini, F. Taddei, M. Polini, and R. Fazio, *Phys. Rev. B* **85**, 144525 (2012); D. Roy, C. J. Bolech, N. Shah, *Phys. Rev. B* **86**, 094503 (2012); M. Wimmer, A. R. Akhmerov, J. P. Dahlhaus, and C. W. J. Beenakker, *New Journal of Physics*, **13**, 053016 (2011); X. -J. Liu, *Phys. Rev. Lett.* **109**, 106404 (2012); C. H. Lin, J. D. Sau, and S. Das Sarma, arXiv:1204.3085; L.-J. Lang, X. M. Cai, and S. Chen, *Phys. Rev. Lett.* **108**, 220401 (2012); L.-J. Lang, S. Chen, *Phys. Rev. B* **86**, 205135 (2012); F. Pientka, G. Kells, A. Romito, P. W. Brouwer, and F. von Oppen, *Phys. Rev. Lett.* **109**, 227006 (2012); D. Bagrets and A. Altland, *Phys. Rev. Lett.* **109**, 227005 (2012); A. Zazunov, A. Levy Yeyati, and R. Egger, *Phys. Rev. B* **84**, 165440 (2011).
- ²² V. L. Berezinskii, *JETP Lett.* **20**, 287 (1974); A. Balatsky and E. Abrahams, *Phys. Rev. B* **45**, 13125 (1992); T. R. Kirkpatrick and D. Belitz, *Phys. Rev. Lett.* **66**, 1533 (1991); M. Vojta and E. Dagotto, *Phys. Rev. B*, **59**, R713 (1999).
- ²³ F. S. Bergeret, A. F. Volkov, and K. B. Efetov, *Phys. Rev. Lett.* **86**, 4096 (2001); Y. Asano, Y. Tanaka, and A. A. Golubov, *Phys. Rev. Lett.* **98**, 107002 (2007); V. Braude and Yu. V. Nazarov, *Phys. Rev. Lett.* **98**, 077003 (2007);
- ²⁴ Y. Tanaka, A. A. Golubov, S. Kashiwaya, and M. Ueda, *Phys. Rev. Lett.* **99**, 037005 (2007); Y. Tanaka, Y. Tanuma, A. A. Golubov, *Phys. Rev. B* **76**, 054522 (2007);
- ²⁵ Y. Tanaka, M. Sato and N. Nagaosa, *J. Phys. Soc. Jpn.* **81**, 011013 (2012).
- ²⁶ L. J. Buchholtz and G. Zwicknagl, *Phys. Rev. B* **23**, 5788 (1981); J. Hara and K. Nagai, *Prog. Theor. Phys.* **74**, 1237 (1986); C. R. Hu, *Phys. Rev. Lett.* **72**, 1526 (1994); S. Kashiwaya and Y. Tanaka, *Rep. Prog. Phys.* **63**, 1641 (2000); Y. Tanaka and S. Kashiwaya, *Phys. Rev. Lett.* **74**, 3451 (1995); Y. Tanaka and S. Kashiwaya, *Phys. Rev. B* **56** 892 (1997), Y. Asano, *Phys. Rev. B* **64**, 014511 (2001); S. Kashiwaya, H. Kashiwaya, H. Kambara, T. Furuta, H. Yaguchi, Y. Tanaka, and Y. Maeno, *Phys. Rev. Lett.* **107**, 077003 (2011).
- ²⁷ Y. Tanaka and A. A. Golubov, *Phys. Rev. Lett.* **98**, 037003 (2007).
- ²⁸ Y. Tanaka, Y. Asano, A. A. Golubov, and S. Kashiwaya, *Phys. Rev. B* **72**, 140503(R) (2005); Y. Tanaka and S. Kashiwaya, *Phys. Rev. B* **70**, 012507 (2004); Y. Tanaka, S. Kashiwaya, and T. Yokoyama, *ibid* **71**, 094513 (2005).
- ²⁹ Y. Tanaka, Yu. V. Nazarov, and S. Kashiwaya, *Phys. Rev. Lett.* **90**, 167003 (2003).
- ³⁰ Y. Asano, Y. Tanaka, and S. Kashiwaya, *Phys. Rev. Lett.* **96**, 097007 (2006).

- ³¹ Y. Asano, Y. Tanaka, A. A. Golubov, and S. Kashiwaya Phys. Rev. Lett. **99**, 067005 (2007).
- ³² Y. Asano, A.A. Golubov, Y. Fominov, and Y. Tanaka, Phys. Rev. Lett. **107**, 087001 (2011).
- ³³ Recent papers have shown that topological superconductivity is stable for weak interactions, S. Gangadharaiah, B. Braunecker, P. Simon, and D. Loss, Phys. Rev. Lett. **107**, 036801 (2011); E. M. Stoudenmire, J. Alicea, O. A. Starykh, and M. P. A. Fisher Phys. Rev. B **84**, 014503 (2011).
- ³⁴ P. A. Lee and D. S. Fisher, Phys. Rev. Lett. **47**, 882 (1981).
- ³⁵ The normal conductance g_N in units of $2e^2/h$ well obeys a relation of $\ln(g_N) \propto -L/\xi_{AL}$ with ξ_{AL} with being the localization length. We estimate that ξ_{AL} for the topological ($V_{ex} = \lambda = 0$) and the non-topological ($V_{ex} = 1.5t, \lambda = 0.5t$) nano wires are about 11 and 8.5 lattice constants, respectively.
- ³⁶ G. E. Blonder, M. Tinkham, and T. M. Klapwijk, Phys. Rev. B **25**, 4515 (1982).
- ³⁷ See Supplemental Material for theoretical details.
- ³⁸ Y. Asano, Y. Tanaka, and S. Kashiwaya, Phys. Rev. B **69**, 214509 (2004).
- ³⁹ J. D. Sau, B. I. Halperin, K. Flensberg, and S. Das Sarma, Phys. Rev. B **84**, 114509 (2011).